Nanographene device fabrication using atomic force microscope

Muneer Ahmad[1], *Yongho Seo*[1,2], *Young Jin Choi*[3]

[1]*Graphene Research Institute, Sejong University, Seoul 143747, Republic of Korea*
[2]*Faculty of Nanotechnology & Advanced Material Engineering and Graphene Research Institute, Sejong University, Seoul 143-747, Republic of Korea*
[3]*Department of Physics, and Department of Nano Science and Engineering, MyongJi University, Yongin 449-728, Republic of Korea*
E-mail: yseo@sejong.ac.kr; jini38@mju.ac.kr

Published in Micro & Nano Letters; Received on 15th April 2013; Accepted on 5th June 2013

A report is presented on the local anodic oxidation of graphene film prepared by chemical vapour deposition using contact mode atomic force microscopy. Raman spectroscopy was used to check the uniformity and thickness of large area graphene film. Various kinds of patterns such as lines, ribbons and further, more complex structures, such as hexagons, two-terminal bar-like devices, were written by varying the tip voltage from −6 to −12 V and the tip speed from 60 to 200 nm/s. It was found that one can easily write any kind of patterns by just manipulating the tip voltage and tip speed instead of concentrating on other factors such as controlled humidity conditions, applied force on the tip and tip current. Also, it is confirmed that with an increase in tip voltage and by slowing the tip movement during lithography, one can write very narrow and sharp patterns which are important factors for the fabrication of graphene-based electronic devices.

1. Introduction: Graphene is a potential candidate as a replacement for traditional silicon in next generation electronic devices [1–3], because of its tremendous range of properties such as extremely high mobility [4, 5], high mechanical strength [6, 7], flexibility and stability at room temperature in spite of the atomic thickness [8, 9]. Therefore it can be used to develop highly efficient carbon-based electronics, but the lack of band gap has made its application challenging, especially for switching devices such as transistors [10, 11]. Conventional electron-beam lithography combined with plasma etching techniques were used to scale down its dimensions to nanoscale but plasma etching introduces defects in graphene, which cause localisation of charge carriers [12, 13]. Therefore we need a new lithography technique which will allow performing atomic resolution patterning without damaging the graphene layer. The scanning probe lithography (SPL), also referred to as atomic force microscopy (AFM)-based local anodic oxidation (LAO), provided a better option because it offers resist-free lithography, thus avoiding contamination of the graphene layer [14–17]. In the beginning, it was applied to silicon [18] and later on used to manipulate metal [19] and graphite [20] surfaces. For graphene nanolithography, already many groups such as Puddy *et al.* [21] and Weng *et al.* [22] have shown precisely written different kinds of patterns by LAO lithography using AFM which can be used to make graphene-based electronic devices. However, many important factors that determine the consistency and resolution of LAO lithography such as tip voltage, tip speed, current, controlled humidity conditions and applied force on the tip are not well established yet for graphene. Especially, the tip voltage for which there is a range (−5 to –35 V) available for graphene nanolithography, is still not standardised [23, 24]. Hence, for realisation of this technique to make graphene-based future nanodevices, more LAO lithographic experiments need to be conducted.

In this reported work, we performed SPM-based lithography using AFM at ambient conditions to precisely write various kinds of patterns such as lines or ribbons, hexagons and two-terminal bar-like devices. The graphene samples used for nanolithography were prepared by the chemical vapour deposition (CVD) technique. In writing these patterns, we manipulated only two key factors, the tip voltage and tip speed, instead of concentrating on other factors such as tip current, controlled humidity conditions and applied force on the tip.

2. Experimental details: Graphene films were grown by the CVD technique on copper foil (25 μm thick, 99.8% purity, Alfa Aesar, item no. 13382) at 950°C in vacuum at a base pressure better than 1×10^{-3} Torr, with a 22 mm inner diameter fused silica tube. The total flow rate of Ar:H_2 was maintained at 250:100 SCCM (cubic centimetre per minute at STP) and 50 SCCM of CH_4 was adopted as the carbon source for all samples. After graphene film deposition, poly (methyl methacrylate) (PMMA) was spin-coated on top of the graphene layer formed on the Cu foil, which was then dissolved in 1 M iron chloride ($FeCl_3$). The resulting graphene/PMMA layer was transferred on to Si/SiO_2 substrates for Raman spectroscopy and LAO lithographic experiments. Raman spectroscopy was conducted using a Renishaw Raman microscope with a laser wavelength of 514 nm. Nanoscale resolution lithography was performed using the commercial AFM (n-Tracer, NanoFocus Inc., South Korea) in contact mode. Electrically conductive Pt/Cr (Multi75E-G) coated probes with spring constant of 3 N/m and resonant frequency of 75 kHz were employed in contact mode for both imaging and lithography purposes. The graphene sample and substrate were grounded and the negative voltage was applied to the tip. Ranges of tip voltages (−6 to −12 V) and tip speeds (60–200 nm/s) were selected for the nanolithography. To apply external negative tip voltage, we used an Advantest-R6144 Programmable DC voltage/current generator. The load on the tip was kept constant as 10 nN in all the measurements and the humidity conditions at room temperature were recorded as 34–40%.

3. Results and discussion: As described above, LAO-based lithography using AFM in contact mode is a better technique than traditional e-beam lithography. Generally, the LAO is performed in air at room temperature with a water meniscus formed between the AFM tip and the sample/substrate as shown in the schematic diagram (Fig. 1*a*). The applied voltage creates an electric field between the tip and the substrate (the substrate needs to be conductive in order to generate the current between the AFM tip and itself), which separates water molecules into H^+ (hydrogen) and OH^- (hydroxyl) ions. When a negative voltage (V_t) is applied to the tip with respect to the sample or substrate which is grounded to the common ground, the graphene surface is oxidised with the help of OH^- ions, which leads to nanopatterning of the graphene [25]. The oxidised graphene surface looks like bumps or holes depending on the voltage. The

doi: 10.1049/mnl.2013.0199

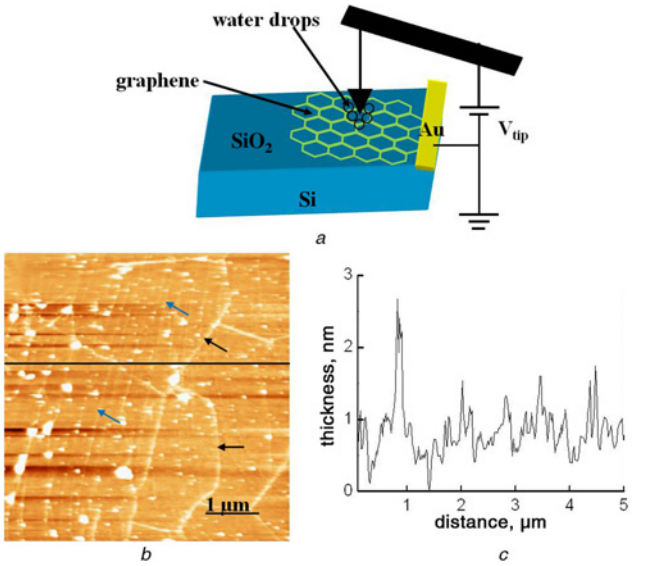

Figure 1 *Fig. 1a: Schematic diagram used to perform LAO lithography. The voltage was applied to the tip in contact mode and the sample/substrate was grounded to the common ground. Fig. 1b: Topography map showing large area CVD grown film with grain boundaries (black) and wrinkles (sky blue) indicated by respective arrows. Fig. 1c: Line profile corresponding to area indicated by black line on topography map of Fig. 1b, giving average thickness of film less than 1 nm*

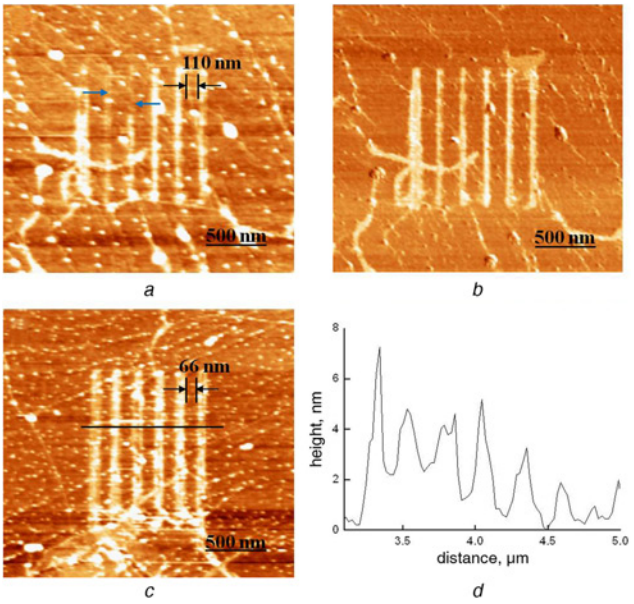

Figure 2 *Fig. 2a: Topography of partially oxidised lines or ribbon patterns obtained by LAO lithography with applied bias −6 V and tip speed 200 nm. Width of graphene trench indicated by black arrows is around 110 nm. Fig. 2b: LFM image taken simultaneously with the topography shows oxidised graphene bumps. Fig. 2c: Topography map illustrating completely oxidised bumps written with increased tip voltage −8 V and by slowing tip movement to 100 nm/s during lithography. Width of graphene trench reduced to 66 nm as indicated by black arrows on topography map of Fig. 2c. Fig. 2d: Line profile corresponds to bumps and trenches created on graphene film along black line on topography map of Fig. 1c*

topography image in Fig. 1*b* obtained by using the setup in Fig. 1*a* shows the large area CVD grown graphene film having average thickness of less than 1 nm, which confirms the single layer as can be observed in the line profile (Fig. 1*c*). The line profile corresponds to the area indicated by the black line on the topography map (Fig. 1*b*). Some high peaks in the line profile may correspond to the dirt particles (white spots) present on the graphene surface as the measurements were performed at ambient conditions. The different sized domain regions (black arrows) and ripples (sky blue arrows) which are typical features of large area CVD grown graphene film can also be observed on the topography image (Fig. 1*b*).

Fig. 2 shows the line or ribbon-like patterns obtained by performing LAO-based lithography with graphene film on Si/SiO_2 substrate. The written patterns that can be seen in the topography map (Fig. 2*a*) as well as clearly distinguishable in the lateral force microscopy image (Fig. 2*b*) were obtained using only the single voltage of −6 V, and the tip speed was 200 nm/s. The width of the obtained patterns indicated by black arrows on the topography map (Fig. 2*a*) is around 110 nm. Some lines specified by sky blue arrows in the topography map (Fig. 2*a*) do not look properly written and appear as just indentations or scratches. To make proper bumps on the selected part of the graphene film during lithography, or in other words, for complete electrical isolation of each line pattern from one another and also to reduce the width of the graphene trench (unpatterned part) than that in the map (Fig. 2*a*), we increased the tip bias to −8 V and reduced the tip speed as 100 nm/s. The topography map in Fig. 2*c* presents the produced patterns under the changed parameters. The selected pattern is well written and the sharp insulating bumps are visible on the oxidised part adjacent to each graphene trench of the patterned graphene. As indicated by black arrows on the topography map (Fig. 2*c*), the width of the patterned trenches of the graphene is reduced by a factor of 44 nm, compared with the width in the topography map (Fig. 2*a*), which is good enough to laterally confine the charge carrier for the opening band gap in the graphene as mentioned by some groups [26, 27]. The line profile in Fig. 2*d* is drawn on the area indicated by the black line on the topography map (Fig. 2*c*) and has maxima and minima that correspond to the bumps and trenches, respectively, created because of LAO of the graphene. Thus, we found that one can easily reduce the dimensions of the graphene trenches and make sharp bumps because of graphene oxidation by just manipulating the tip voltage and tip speed at ambient conditions instead of concentrating on other parameters such as humidity, tip current or force on the tip as mentioned by Puddy *et al.* [21].

Then, we tried LAO to write horizontal lines or ribbons blocked from one end alternatively and intentionally as indicated by the sky blue arrows on the LFM map (Fig. 3*b*) and topography map (Fig. 3*c*) in Fig. 3. The tip voltage and tip speed used to write these patterns was −7 V and 100 nm/s, respectively. As can be observed from the topography map (Fig. 3*a*), there is no visible sign of a written pattern but in the LFM image (Fig. 3*b*) scratches like lines can be observed, which might be because of partial oxidation of the selected region of the graphene film for lithography. To make proper oxidised graphene bumps, we again tried a similar kind of pattern by increasing the tip bias to −9 V and keeping the same speed as that in the LFM map (Fig. 3*b*). We can see sharp written patterns having bumps created on the oxidised part clearly distinguishable on both the topography (Fig. 3*c*) as well as LFM (Fig. 3*d*) maps. This kind of narrow width lithographic patterns of graphene can also be used as channels blocked from one end to confine the charge carriers to nanodimensions for surface conductivity studies at the defect sites of nanosize [28]. One important thing to be noted here is that, for use of graphene in device fabrication by LAO, AFM height imaging is not enough to establish the difference between electrically isolated bumps of oxidised graphene and the trenches which correspond to the graphene devices. For this purpose, we need to perform either the charge transport measurements or conductive AFM studies. This is because the ability to differentiate between actual electrical isolation and just scratches is very important for device fabrication of graphene.

Next, we write some complex patterns such as hexagons, two-terminal bar-shaped devices and so on. For this task, we increased

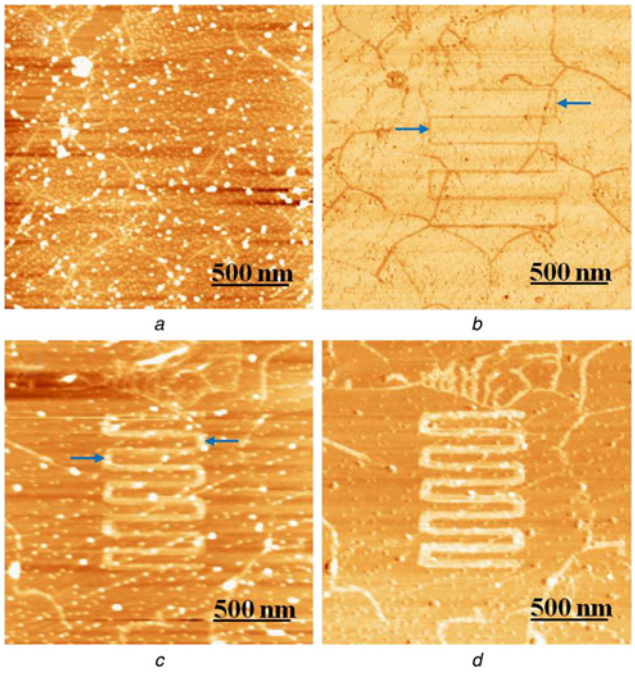

Figure 3 *Horizontal lines or ribbon patterns closed from one end alternatively were selected to write in topography map*
a As slightly patterned lines can be seen in LFM map
b Produced during LAO lithography performed with applied bias −7 V and tip speed 100 nm/s
c Topography map and LFM map
d Clearly distinguish thick patterns written with increased voltage −9 V and tip speed 100 nm/s
Sky blue arrows in LFM map of Fig. 3*b* as well as in topography map of Fig. 3*c* point towards intentionally alternatively written closed ends

the tip voltage to −10 V and the tip speed was slowed down to 60 nm/s for reliable writing of complicated patterns. First, we selected a hexagon-like structure as presented in the topography map. Fig. 4*a* is not well visible maybe because of the low resolution of the image, but the LFM map (Fig. 4*b*) shows a clearly written pattern as the frictional forces are more sensitive than AFM [29]. We increased the number of hexagons connected together to write more complex patterns simultaneously by using the same voltage and tip speed as used for the pattern map of Fig. 4*a* and the developed pattern is presented in the topography map of Fig. 4*c*. Almost all the selected portion is oxidised except at some points (indicated by black arrows) as the bumps because of oxidation are not properly distinguishable. This may have happened owing to the applied bias not being enough for this more complex structure because of which graphene is partially oxidised which leads to just scratches on some parts, or may be because of the low resolution of the oxidised bumps as a lot of dirt particles (white spots) are present on the graphene surface. However, if we look at the LFM map (Fig. 4*d*), all the hexagons appear well developed because of LAO-based lithography. Subsequently, we selected to write a two-terminal bar-like device pattern which can directly be used for electrical measurements. The tip voltage was increased to −12 V, and with the same tip speed 60 nm/s, the two-terminal bar-like device written can be seen in the topography map (Fig. 4*e*). The bumps and trenches produced on the graphene film are clearly distinguishable in both the topography (Fig. 4*e*) and the LFM (Fig. 4*f*) images. The width of the device is around 36 nm, as indicated by black arrows on the topography map (Fig. 4*e*). The device looks blocked from the right side indicated by the sky blue arrow on the topography map (Fig. 4*e*) as the unwanted graphene portion is oxidised unintentionally. This may have happened because of the uncontrolled movement of the tip during lithography as the voltage source used for this pattern was

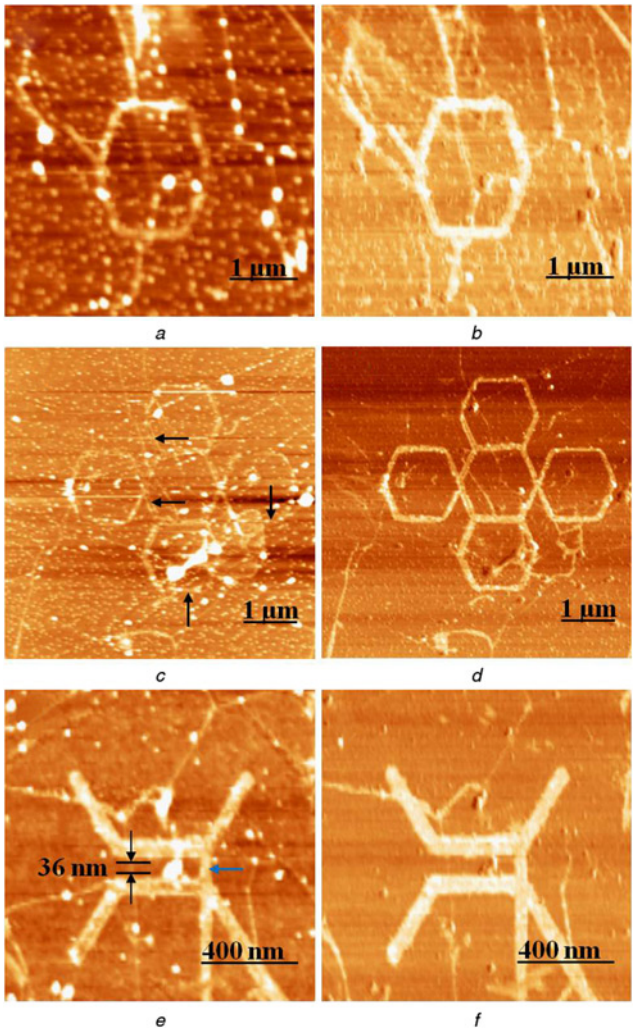

Figure 4 *Figs. 4a and b: Topography and LFM maps, respectively, presenting hexagon-like complex pattern written by LAO lithography with applied bias −10 V and tip speed 60 nm/s. More hexagons were written simultaneously as presented in topography (partially visible) map of Fig. 4c and are clearly distinguishable in LFM map of Fig. 4d. Voltage and tip speed used to write these hexagons was same as for topography map of Fig. 4d. Two-terminal device-like pattern was written having device width 36 nm (indicated by black arrows) with applied voltage −12 V and tip speed 60 nm/s as presented in topography map of Fig. 4e as well as in LFM map of Fig. 4f*
Sky blue arrow on right of image indicates unintentional blocking of device

external voltage source, instead of internal source (maximum limit −10 V) from within the system as for earlier patterns which is synchronised with the tip movement. The range of voltages (−6 to −12 V) selected for our experiments was below the middle range in comparison to the values (−6 to −35 V) reported by other groups as discussed in the Introduction Section. Hence, by using a moderate voltage range, we have shown that any kind of pattern can be simply obtained at room temperature. The important thing to take care of in making stable cuts regarding tip voltage is that the voltage levels to be used for LAO lithography should be sufficiently high, because the trenches made with small voltages will fade away with time and recover the original shape [21]. Finally, we confirm that the promise of the LAO lithography technique described here is well suited for the fabrication of nanoscale resolution graphene-based electronic devices. The convenience of performing the LAO lithography we proposed in this Letter, is that by just manipulating the tip bias and tip speed, one can simply write any kind of pattern at room temperature instead of concentrating on other factors as addressed by some authors discussed

doi: 10.1049/mnl.2013.0199

above. Our findings will hopefully contribute to the designing of graphene-based electronic devices by LAO-based lithography using AFM.

4. Conclusion: We have performed LAO lithography on single layer graphene prepared by CVD using AFM. By writing many patterns such as lines, ribbons and more complex structures, such as hexagons, two-terminal bar-like devices, we have shown that any kind of lithographic pattern for the lateral confinement of charge carriers in graphene can be written by just manipulating the tip voltage and tip speed instead of concentrating on other parameters. We have shown that the narrowing of the graphene trench and the sharpness of oxidised insulating bumps can be achieved by increasing the tip voltage and lowering the tip speed. The experimental results presented in this Letter regarding LAO-based patterning using AFM confirm that it is an effective technique for fabricating graphene-based future electronic devices.

5. Acknowledgments: This research was supported by the Basic Science Research Program (2009-0070725, 2010-0005393) and the Priority Research Centers Program (2012-0005859) through the NRF funded by MEST.

6 References

[1] Castro Neto A.H., Peres N.M.R., Novoselov K.S., Geim A.K.: 'The electronic properties of graphene', *Rev. Modern Phys.*, 2009, **81**, (1), pp. 109–162

[2] Geim A.K.: 'Graphene: status and prospects', *Science*, 2009, **324**, (5934), pp. 1530–1534

[3] Ahmadi S., Esmaeilzadeh M.: 'Effects of electrostatic potential on spin-inversion in nano-scale graphene sheets with a single Rashba spin-orbit barrier', *Micro Nano Lett.*, 2012, **7**, (8), pp. 790–794

[4] Lu C.-C., Lin Y.-C., Yeh C.-H., Huang J.-C., Chiu P.-W.: 'High mobility flexible graphene field-effect transistors with self-healing gate dielectrics', *ACS Nano*, 2012, **6**, pp. 4469–4474

[5] Wang S., Ang P.K., Wang Z., Tang A.L., Thong J.T., Loh K.P.: 'High mobility, printable, and solution-processed graphene electronics', *Nano Lett.*, 2010, **10**, (1), pp. 92–98

[6] Min K., Aluru N.R.: 'Mechanical properties of graphene under shear deformation', *Appl. Phys. Lett.*, 2011, **98**, (1), p. 013113

[7] Ranjbartoreh A.R., Wang B., Shen X.P., Wang G.X.: 'Advanced mechanical properties of graphene paper', *J. Appl. Phys.*, 2011, **109**, (1), p. 014306

[8] Chen Z.P., Ren W.C., Gao L.B., Liu B.L., Pei S.F., Cheng H.M.: 'Three-dimensional flexible and conductive interconnected graphene networks grown by chemical vapour deposition', *Nat. Mater.*, 2011, **10**, (6), pp. 424–428

[9] Sui D., Huang Y., Huang L., Liang J., Ma Y., Chen Y.: 'Flexible and transparent electrothermal film heaters based on graphene materials', *Small*, 2011, **7**, (22), pp. 3186–3192

[10] Seo Y., Cadden-Zimansky P., Chandrasekhar V.: 'Low-temperature scanning force microscopy using a tuning fork transducer', *J. Korean Phys. Soc.*, 2007, **50**, (2), pp. 378–383

[11] Balog R., Jorgensen B., Nilsson L., *ET AL.*: 'Bandgap opening in graphene induced by patterned hydrogen adsorption', *Nat. Mater.*, 2010, **9**, (4), pp. 315–319

[12] Song H.S., Li S.L., Miyazaki H., *ET AL.*: 'Origin of the relatively low transport mobility of graphene grown through chemical vapor deposition', *Sci. Rep.*, 2012, **2**, pp. 337

[13] Childres I., Jauregui L.A., Tian J., Chen Y.P.: 'Effect of oxygen plasma etching on graphene studied using Raman spectroscopy and electronic transport measurements', *New J. Phys.*, 2011, **13**, (2), p. 025008

[14] Alaboson J.M., Wang Q.H., Kellar J.A., *ET AL.*: 'Conductive atomic force microscope nanopatterning of epitaxial graphene on Sic (0001) in ambient conditions', *Adv. Mater.*, 2011, **23**, (19), pp. 2181–2184

[15] Biró L.P., Lambin P.: 'Nanopatterning of graphene with crystallographic orientation control', *Carbon*, 2010, **48**, (10), pp. 2677–2689

[16] He Y., Dong H., Li T., Wang C., *ET AL.*: 'Graphene and graphene oxide nanogap electrodes fabricated by atomic force microscopy nanolithography', *Appl. Phys. Lett.*, 2010, **97**, (13), p. 133301

[17] Yong H., Kim K., Choi W., Park J., Ahmad M., Seo Y.: 'The production of a cellular graphene array by scanning probe lithography and its ability to store electrical charge', *Carbon*, 2012, **50**, (12), pp. 4640–4647

[18] Snow E.S., Campbell P.M.: 'Fabrication of SI nanostructures with an atomic-force microscope', *Appl. Phys. Lett.*, 1994, **64**, (15), pp. 1932–1934

[19] Snow E.S., Park D., Campbell P.M.: 'Single-atom point contact devices fabricated with an atomic force microscope', *Appl. Phys. Lett.*, 1996, **69**, (2), p. 269

[20] Albrecht T.R., Dovek M.M., Kirk M.D., Lang C.A., Quate C.F., Smith D.P.E.: 'Nanometer-scale hole formation on graphite using a scanning tunneling microscope', *Appl. Phys. Lett.*, 1989, **55**, (17), pp. 1727–1729

[21] Puddy R.K., Scard P.H., Tyndall D., *ET AL.*: 'Atomic force microscope nanolithography of graphene: cuts, pseudocuts, and tip current measurements', *Appl. Phys. Lett.*, 2011, **98**, (13), p. 133120

[22] Weng L.S., Zhang L.Y., Chen Y.P., Rokhinson L.P.: 'Atomic force microscope local oxidation nanolithography of graphene', *Appl. Phys. Lett.*, 2008, **93**, (9), p. 093107

[23] Neubeck S., Ponomarenko L.A., Freitag F., *ET AL.*: 'From one electron to one hole: quasiparticle counting in graphene quantum dots determined by electrochemical and plasma etching', *Small*, 2010, **6**, (14), pp. 1469–1473

[24] Masubuchi S., Ono M., Yoshida K., Hirakawa K., Machida T.: 'Fabrication of graphene nanoribbon by local anodic oxidation lithography using atomic force microscope', *Appl. Phys. Lett.*, 2009, **94**, (8), pp. 082107–082103

[25] Masubuchi S., Arai M., Machida T.: 'Atomic force microscopy based tunable local anodic oxidation of graphene', *Nano Lett.*, 2011, **11**, (11), pp. 4542–4546

[26] Neubeck S., Freitag F., Yang R., Novoselov K.S.: 'Scanning probe lithography on graphene', *Physica Status Solidi B*, 2010, **247**, (11–12), pp. 2904–2908

[27] Lu G., Zhou X., Li H., *ET AL.*: 'Nanolithography of single-layer graphene oxide films by atomic force microscopy', *Langmuir*, 2010, **26**, (9), pp. 6164–6166

[28] Ahmad M., An H., Kim Y.S., *ET AL.*: 'Nanoscale investigation of charge transport at the grain boundaries and wrinkles in graphene film', *Nanotechnology*, 2012, **23**, (28), p. 285705

[29] Lee H., Lee N., Seo Y., Eom J., Lee S.: 'Comparison of frictional forces on graphene and graphite', *Nanotechnology*, 2009, **20**, (32), p. 325701